Non-Destructive Testing of Thermal Resistances for a Single Inclusion in a 2-Dimensional Domain

Nicholas Christian* and Mathew A. Johnson†

September 5, 2004

Abstract

In this paper we examine the inverse problem of determining the amount of corrosion/disbonding which has occurred on the boundary of a single circular (or nearly circular) inclusion D in a two-dimensional domain Ω, using Cauchy data for the steady-state heat equation. We develop an algorithm for reconstructing a function which quantifies the level of corrosion/disbonding at each point on ∂D. We also address the issue of ill-posedness and develop a simple regularization scheme, then provide several numerical examples. We also show a simple procedure for recovering the center of D assuming that Ω and D have the same thermal conductivity.

*University of North Carolina at Asheville
†Ball State University

1 Introduction

The ability to determine whether there are any defects on the interior of an object without destroying it is an invaluable tool in today's industry. Two popular methods for this are steady state thermal imaging and impendence imaging, both of which are governed by the same basic mathematical equations, used throughout this paper: the physical interpretation must be adjusted to meet the given circumstance. We will use the thermal terminology.

This paper outlines a process in which steady state heat flow is used to determine the constitutive law governing how a single inclusion in an object impedes the flow of heat. In particular, we will be concerned with circular or nearly circular disks D encapsulated inside an outer region Ω. Our goal is to produce a function which quantifies the behavior of the heat flow across the interface between Ω and D. That is, as we move along the inclusion's boundary ∂D, we want to know at any particular point how much heat flow is being impeded—we treat the interface ∂D as a kind of "contact resistance". Initially we consider the region D itself as known. The goal is to recover the contact resistance over ∂D; here we are thinking of a composite material with known geometry (D is known) but with possible corrosion at the material interface. From knowing the thermal properties at ∂D we hope to make inferences as to how much disbonding or corrosion has occurred on the interface between Ω and D. We will also examine the problem of finding the location of the inclusion D in the case where Ω and D have the same thermal conductivity.

2 The Forward Problem

Let Ω be a bounded region in $\mathbb{R}^2$ with boundary $\partial\Omega$. We assume, after appropriate scaling, that Ω has thermal conductivity and diffusivity equal to one. Let $D \subset \Omega$ be an inclusion with presumably different thermal properties from those of Ω - say D has conductivity α and diffusivity κ, both considered known. A time independent heat flux g is applied to $\partial\Omega$ for some time; we assume this time is long enough so that the temperature inside Ω stabilizes at some function $u(x, y)$. Then we assume the function u satisfies the 2-dimensional steady state heat equation

$$\Delta u(x, y) \ := \ \frac{\partial^2 u}{\partial x^2} + \frac{\partial^2 u}{\partial y^2} = 0 \tag{1}$$

in $\Omega \setminus D$ and D, as well as the boundary condition

$$\frac{\partial u}{\partial \mathbf{n}}(\mathbf{p}) \ = \ \nabla u(\mathbf{p}) \cdot \mathbf{n}(\mathbf{p}) \ = \ g(\mathbf{p}) \tag{2}$$

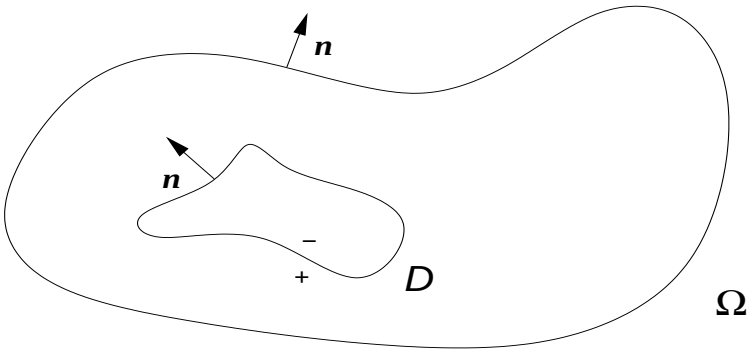

Figure 1: A diagram of a 2-D region Ω with a single inclusion D.

for $\mathbf{p} \in \partial\Omega$, where $\mathbf{n}$ is a unit outward normal vector on $\partial\Omega$ and Δ is known as the Laplacian. Functions which solve (1) are said to be harmonic in $\Omega \setminus D$ and D, and they are of great importance in several areas of mathematics and physics.

Throughout this paper, we will use a superscript "+" to denote the limiting value of a quantity as approached from outside D, and a superscript "-" to denote the limiting value of a quantity as approached from inside D. Let us first suppose the interface ∂D between the two regions $\Omega \setminus D$ and D is uncorroded. Then we would have $[u](\mathbf{p}) = 0$ for all $\mathbf{p} \in \partial D$, where $[u](\mathbf{p}) = u^+(\mathbf{p}) - u^-(\mathbf{p})$ is the jump in u over ∂D. In short, u should be continuous across ∂D. We should also require that the rate at which energy flows past $\mathbf{p}$ from inside D equals the rate at which energy flows past $\mathbf{p}$ from outside D, *i.e.*, conservation of energy. This can be quantified as

$$\frac{\partial u^+}{\partial \mathbf{n}}(\mathbf{p}) = \alpha \frac{\partial u^-}{\partial \mathbf{n}}(\mathbf{p}), \quad \mathbf{p} \in \partial D$$

where $\mathbf{n}$ is a unit outward normal vector on ∂D.

Now suppose that ∂D has corroded or disbonded. We expect this would manifest

itself as some type of thermal contact resistance to the flow of heat over ∂D. We model this contact resistance as

$$\frac{\partial u^+}{\partial \mathbf{n}}(\mathbf{p}) = k(\mathbf{p})[u](\mathbf{p}) = \alpha \frac{\partial u^-}{\partial \mathbf{n}}(\mathbf{p}),\ \mathbf{p} \in \partial D \tag{3}$$

for some function $k(\mathbf{p}) \geq 0$ which quantifies the magnitude of the contact resistance across ∂D. The case where $k \equiv 0$ implies no heat flows over ∂D and thus we have a complete disbond. Note that since we don't expect that the corrosion levels will be the same at every point on the boundary of the inclusion, k is required to be a function of position.

The forward problem presented above involves solving for the steady temperature $u(x, y)$ given that u satisfies the Neumann boundary value problem (1)-(3) and that the flux g is known. This problem has a unique solution, up to an additive constant: to ensure a unique solution, we add the normalization condition $\int_{\partial\Omega} u\, ds = 0$. The forward problem will not, however, be the object of our analysis. We will instead be interested in the following inverse problem: given the solution u to (1)-(3) on $\partial\Omega$, with g being a given, determine the function k in (3).

3 Preliminaries

We begin with a two-dimensional domain Ω and a single inclusion D completely contained inside Ω. Let us recall Green's second identity: for any bounded region $\Gamma \subset \mathbb{R}^2$, with sufficiently smooth boundary $\partial\Gamma$, if $u,\ v \in C^2(\Gamma \cup \partial\Gamma)$, then

$$\int\int_{\Gamma} (u\Delta v\ -\ v\Delta u)\, dA\ \ =\ \ \int_{\partial\Gamma} \left(u\frac{\partial v}{\partial \mathbf{n}}\ -\ v\frac{\partial u}{\partial \mathbf{n}} \right)\, ds \tag{4}$$

where ds represents an element of arc-length and $\mathbf{n}$ is a unit outward normal to $\partial\Gamma$ (see [4]). This identity is a direct consequence of the Divergence Theorem and will be the driving force for recovering the needed information to reconstruct k.

Due to the geometry of the problem, we will utilize polar coordinates for most of our computations. For simplicity, we will assume Ω is the unit disk. We will take the origin of our coordinate system to be the center of Ω and let (r, θ) be a point in Ω in standard polar coordinates (this will make our numerical computations much easier later, although they would be doable for any domain Ω with a smooth boundary). Let D have radius R_D and have its center at the point (x_0, y_0). Also, let (ρ, β) represent polar coordinates as if the center of our coordinate system was

(x_0, y_0). In our (r, θ) coordinate system, (1) and (2) become

$$\Delta u(r,\theta) = \frac{1}{r}\frac{\partial}{\partial r}\left(r\frac{\partial u}{\partial r}\right) \;+\; \frac{1}{r^2}\frac{\partial^2 u}{\partial \theta^2} = 0 \text{ in } \Omega \setminus D \text{ and } D \tag{5}$$

$$\frac{\partial u}{\partial r} \;=\; g(1,\theta) \tag{6}$$

We also need to recall the basic definition of a Fourier series: if $f(x)$ is a piecewise-smooth, 2π-periodic continuous function defined on the interval $[-\pi, \pi]$, it can be represented as a Fourier series on that interval as

$$f(x) \;=\; \frac{a_0(f)}{2} \;+\; \sum_{n=1}^{\infty} \left(a_n(f)\cos(nx) \;+\; b_n(f)\sin(nx)\right) \tag{7}$$

where the Fourier coefficients are given by

$$a_n(f) \;=\; \frac{1}{\pi}\int_{-\pi}^{\pi} f(x)\cos(nx)\,dx, \quad \text{for } n \geq 0,$$

$$b_n(f) \;=\; \frac{1}{\pi}\int_{-\pi}^{\pi} f(x)\sin(nx)\,dx, \quad \text{for } n \geq 1.$$

4 Recovering k(p)

Our goal in this section is to reconstruct the flux $\frac{\partial u^+}{\partial \mathbf{n}}$ and the jump $[u]$ independently as Fourier series, in order to isolate the function k from (3). Classically, we would be given a function and asked to reconstruct it as a Fourier series using the above definitions. However, we cannot do this directly since we do not know the function we are trying to reconstruct (that's the whole point!). So how can we recover the Fourier coefficients of an unknown function?

The answer is to make clever use of Green's second identity. Let $u(r, \theta)$ be a solution to (5) and (6) and let $v(r, \theta)$ be any function harmonic on $\Omega \setminus D$. Applying (4) to $\Omega \setminus D$, keeping in mind that $\mathbf{n}$ represents a unit outward normal, we have

$$\int_{\partial\Omega}\left(u\frac{\partial v}{\partial \mathbf{n}} \;-\; v\,g\right)\,ds \;-\; \int_{\partial D}\left(u^+\frac{\partial v}{\partial \mathbf{n}} \;-\; v\frac{\partial u^+}{\partial \mathbf{n}}\right)\,ds = 0.$$

The first integral above (over $\partial\Omega$) is often referred to as the reciprocity gap integral, and is denoted hereafter as $RG(v)$. Note that this is a linear operator and is computable for any function v harmonic in $\Omega \setminus D$ from the known boundary data for u.

This gives us our following powerful identity:

$$RG(v) = \int_{\partial D} \left(u^+ \frac{\partial v}{\partial \mathbf{n}} - v \frac{\partial u^+}{\partial \mathbf{n}} \right) ds. \tag{8}$$

This identity has been used extensively in examining the problem of finding the location and constitutive law governing heat flow across a crack σ in a domain Ω, and we refer the reader to [2] and the references therein for more information.

Notice that in (8) we are free to use *any* harmonic test function we choose. Therefore, we will use specifically designed test functions to extract the Fourier coefficients of the flux, as well as the jump. With this information in hand, we can reconstruct the flux and the jump on ∂D, as in (7), and thus determine the function k. We first start with recovering the flux in u across ∂D.

4.1 Recovering the Flux

As described above, we wish to design a certain family of test functions $v_n(r, \theta)$ from which we can use (8) to extract the Fourier coefficients of $\frac{\partial u^+}{\partial \mathbf{n}}$ on the interval $[-\pi, \pi]$. Such test functions would have to be harmonic in $\Omega \setminus D$ (that is, satisfy equation (5)) in order for (8) to be valid. Note that since D is a circle, the normal derivative of v_n on ∂D is simply the radial derivative in the (ρ, β) coordinate system. By examining (8),we wish for our test functions to take the form of a sine or cosine and have a zero radial derivative on ∂D. One can easily verify by direct substitution that the following families of test functions satisfy these properties for any positive integer n:

$$v_n^c(\rho, \beta) = \left(\rho^n + R_D^{2n} \rho^{-n}\right) \cos(n\beta) \tag{9}$$

$$v_n^s(\rho, \beta) = \left(\rho^n + R_D^{2n} \rho^{-n}\right) \sin(n\beta) \tag{10}$$

where we recall that R_D is the radius of D. Substituting (9) into equation (8) yields (since $ds = R\, d\beta$)

$$RG(v_n^c) = -\int_{\partial D} 2R_D^n \frac{\partial u^+}{\partial \mathbf{n}} \cos(n\beta) ds = -2R_D^{n+1} \int_{-\pi}^{\pi} \frac{\partial u^+}{\partial \mathbf{n}} \cos(n\beta) d\beta.$$

Similar computations can be carried out for v_n^s. Therefore, we have that the Fourier sine and cosine coefficients of $\frac{\partial u^+}{\partial \mathbf{n}}$ are given by

$$a_n \left(\frac{\partial u^+}{\partial \mathbf{n}} \right) = \frac{1}{\pi} \int_{-\pi}^{\pi} \frac{\partial u^+}{\partial \mathbf{n}} \cos(n\beta) d\beta = \frac{-RG(v_n^c)}{2\pi R_D^{n+1}}, \text{ n} \geq 0 \tag{11}$$

$$b_n \left(\frac{\partial u^+}{\partial \mathbf{n}} \right) = \frac{1}{\pi} \int_{-\pi}^{\pi} \frac{\partial u^+}{\partial \mathbf{n}} \sin(n\beta) d\beta = \frac{-RG(v_n^s)}{2\pi R_D^{n+1}}, \text{ n} \geq 1 \tag{12}$$

respectively. We have thus reconstructed the flux across ∂D as

$$\frac{\partial u^+}{\partial \mathbf{n}}(R_D,\beta) = \frac{a_0\left(\frac{\partial u^+}{\partial \mathbf{n}}\right)}{2} + \sum_{n=1}^{\infty}\left(a_n\left(\frac{\partial u^+}{\partial \mathbf{n}}\right)\cos(n\beta) + b_n\left(\frac{\partial u^+}{\partial \mathbf{n}}\right)\sin(n\beta)\right) \quad (13)$$

in the (ρ,β) coordinate system. Note that from (3), we have now solved for the quantity $k(\beta)[u](\beta)$. If we determine $[u]$ we will have recovered k.

4.2 Recovering the Temperature Jump

To recover the jump we will recover u^+ and u^- separately, then take their difference (recall that $[u] = u^+ - u^-$). In order to recover u^+, we turn back to equation (8). We wish to design a family of test functions q_n which are harmonic in $\Omega \setminus D$, equal to zero on ∂D, and whose radial derivative takes the form of a sine or cosine on ∂D. Again, one can verify by direct substitution that the functions defined by

$$q_n^c(\rho,\beta) = \left(\rho^n - R_D^{2n}\rho^{-n}\right)\cos(n\beta), \quad (14)$$

$$q_n^s(\rho,\beta) = \left(\rho^n - R_D^{2n}\rho^{-n}\right)\sin(n\beta), \quad (15)$$

satisfy these properties for any positive integer n. By substituting (14) and (15) into (8), we see that the Fourier sine and cosine coefficients for u^+ are given by

$$a_n\left(u^+\right) = \frac{1}{\pi}\int_{-\pi}^{\pi} u^+\cos(n\beta)d\beta = \frac{RG(q_n^c)}{2n\pi R_D^n},\ \text{n} \geq 1 \quad (16)$$

$$b_n\left(u^+\right) = \frac{1}{\pi}\int_{-\pi}^{\pi} u^+\sin(n\beta)d\beta = \frac{RG(q_n^s)}{2n\pi R_D^n},\ \text{n} \geq 1 \quad (17)$$

respectively. Notice that we have determined each of the coefficients except for $a_0(u^+)$. We'll address this issue after we recover u^-. For now, we'll consider the quantity u^+ as known.

We now need only to recover u^-. We can not use equation (8) here since our u^- doesn't appear in that equation. We slightly adapt the above procedure by applying Green's second identity to D and see that for any function v harmonic in D we have

$$\int_{\partial D} u^-\frac{\partial v}{\partial \mathbf{n}}ds = \int_{\partial D} v\frac{\partial u^-}{\partial \mathbf{n}}ds. \quad (18)$$

Define the following families of test functions

$$z_n^c(\rho,\beta) = \alpha\rho^n\cos(n\beta) \quad (19)$$

$$z_n^s(\rho,\beta) = \alpha\rho^n\sin(n\beta) \quad (20)$$

for any positive integer n where α is the (known) thermal conductivity of D. Substitution into (18) yields

$$\int_{\partial D} R_D^{n-1} \alpha n u^- \cos(n\beta) ds = \int_{\partial D} R_D^n \alpha \frac{\partial u^-}{\partial \mathbf{n}} \cos(n\beta) ds.$$

Upon recalling equation (3) this becomes

$$\begin{aligned} \int_{\partial D} R_D^{n-1} \alpha n u^- \cos(n\beta) ds &= \int_{\partial D} R_D^n \frac{\partial u^+}{\partial \mathbf{n}} \cos(n\beta) ds \\ &= \pi R_D^{n+1} a_n \left(\frac{\partial u^+}{\partial \mathbf{n}} \right) \\ &= \frac{-RG(v_n^c)}{2} \end{aligned}$$

by (11). A similar computation can be carried out for z_n^s. Therefore, the Fourier cosine and sine coefficients of u^- are given by

$$a_n\left(u^-\right) = \frac{1}{\pi} \int_{-\pi}^{\pi} u^- \cos(n\beta) d\beta = \frac{-RG(v_n^c)}{2n\pi\alpha\ R_D^n},\ \mathrm{n} \geq 1 \tag{21}$$

$$b_n\left(u^-\right) = \frac{1}{\pi} \int_{-\pi}^{\pi} u^- \sin(n\beta) d\beta = \frac{-RG(v_n^s)}{2n\pi\alpha R_D^n},\ \mathrm{n} \geq 1 \tag{22}$$

respectively. Note again that we have no information about $a_0(u^-)$. However, we will consider the quantity u^- as being known, up to an additive constant.

We are now in position to reconstruct $[u]$. By subtracting the coefficients term by term, we see that we can represent the jump as

$$[u](\beta) = \frac{A_0}{2} + \sum_{n=1}^{\infty} \left(A_n \cos(n\beta) + B_n \sin(n\beta) \right) \tag{23}$$

with coefficients

$$A_n = \frac{RG(w_n^c)}{2n\pi R_D^n},\ \mathrm{n} \geq 1, \tag{24}$$

$$B_n = \frac{RG(w_n^s)}{2n\pi R_D^n},\ \mathrm{n} \geq 1 \tag{25}$$

where

$$w_n^c(\rho,\beta) = q_n^c(\rho,\beta) + \frac{1}{\alpha} z_n^c(\rho,\beta) = \left[\left(\frac{1}{\alpha} + 1 \right) \rho^n + \left(\frac{1}{\alpha} - 1 \right) R_D^{2n} \rho^{-n} \right] \cos(n\beta),$$

and the function w_n^s is defined similarly. We have thus recovered all of the information necessary to reconstruct $k(\beta)$, except for the constant term (since we have no information about $a_0(u^+)$ or $a_0(u^-)$).

To determine the constant term $\frac{A_0}{2}$ above, we recall that for any given β we have $k(\beta) \geq 0$. In (13) we showed the complete reconstruction of the product $k(\beta)[u](\beta)$. By conservation of energy, we know that the net amount of energy entering and leaving D must be the same, which forces

$$\int_{\partial D} \frac{\partial u^+}{\partial \mathbf{n}}\, ds = 0. \tag{26}$$

If the flux across ∂D is not identically zero (which can't happen if g is not identically zero) then from (26) we know that $\frac{\partial u^+}{\partial \mathbf{n}}$ must change signs at least once in the interval $[-\pi, \pi]$. Since k is non-negative, this implies that $[u]$ must change signs at the same point that the flux does. It's easy to see that this uniquely determines the value of our unknown constant (compute $[u]$ via equation (23) with an undetermined value for A_0, then adjust A_0 so that $[u](\beta^*) = 0$, where β^* is any point at which $\frac{\partial u^+}{\partial \mathbf{n}}(\beta^*) = 0$). Thus we have completely recovered the jump.

We now have all the information to compute $k(\beta)$: given $\beta \in [-\pi, \pi]$, one can compute the flux at that angle, as well as the jump via (13) and (23), with $\frac{A_0}{2}$ computed as above. Dividing the flux by the jump, assuming $[u] \neq 0$, will then give k at the specified angle.

4.3 Generalization

The requirement made by (3) was nothing more than a special case of a more general constitutive law which might hold on the boundary of D. The above procedure can be easily generalized to the case where (3) is replaced by

$$\frac{\partial u^+}{\partial \mathbf{n}}(\mathbf{p}) \;=\; F\left(\mathbf{p}, [u](\mathbf{p})\right) \text{ for } \mathbf{p} \in \partial D,$$

where we require that $F(0) = 0$, F is a non-decreasing odd function (and in practice, strictly increasing), and continuous. The reason for this is that heat flows in proportion to the temperature difference (from higher temperatures to lower temperatures). If there is no temperature difference at the boundary of the inclusion D, then no heat should flow through it and thus $F(0) = 0$. When the jump is positive at a point $p \in \partial D$, the temperature on the exterior of the inclusion is higher than the temperature on the interior of the inclusion in a small neighborhood of p. This

implies that the heat flow should be positive. So, the larger the temperature jump at p, the greater the heat flow should be through it. Therefore, F should be required to be non-decreasing as a function of $[u]$. The reason for F being odd is simple: if you have a jump $[u]_0$ and flux F_0 at a point, then you would expect $F(-[u]_0)$ to have the same magnitude, but the heat should flow in the opposite direction giving $F(-[u]_0) = -F_0$. Hence, F should be odd.

The generalization to recover the unknown function F is simple. Since we can recover the flux and the jump on ∂D, by evaluating each of them at an angle $\beta \in [-\pi, \pi]$, we know that

$$\frac{\partial u^+}{\partial \mathbf{n}}(\beta) \;=\; F\left([u](\beta)\right).$$

Therefore, we can reconstruct the function F on the set of all temperature jumps on ∂D without any modification to the above procedure.

5 Numerical Implementation

With the theory just developed as the foundation, we wrote a program which will numerically solve the inverse problem described above where Ω is the unit disk. In what follows, we discuss the program we designed and use it to solve a particular instance of the inverse problem. We will analyze our results to try to gain insight into the behavior of the inverse problem. In this section we assume the data has no noise (noisy data and a strategy for dealing with the ill-posedness will be discussed in the next section).

5.1 Approximations and Consequences

Before we implement the above procedure, we first need to address some issues of practicality. Our procedure involves computing two infinite series of trigonometric functions. Obviously we can't compute the full series, and so must truncate our expansions for the jump as well as the flux across ∂D. This will immediately introduce error into our reconstruction of k.

To analyze to what extent this error will manifest itself, we will consider the Fourier series expansion of a general function f defined on $[-\pi, \pi]$. Let $\tilde{f}_N$ represent the Fourier series representation of f truncated at $n = N \geq 1$, *i.e.*,

$$\tilde{f}_N(x) = \frac{a_0}{2} + \sum_{j=1}^{N} \left(a_n \cos(jx) + b_n \sin(jx)\right) \tag{27}$$

We wish to measure the error in using this truncated approximation the function f. One useful way to measure this would be by using the L^2 norm of the difference $f - \tilde{f}_N$ (this in essence measures the distance between the two functions). Recall that if $g \in L^2((a,b))$, *i.e.*, $\int_a^b g^2(t)dt < \infty$, then the L^2 norm of g on (a,b) is given by

$$|g|_2 = \left(\int_a^b g^2(x)dx \right)^{1/2}.$$

Also, recall Parseval's identity which states that if a function g is represented as a Fourier series as in equation (7), then

$$|g|_2^2 = \frac{a_0^2(g)}{2} + \sum_{n=1}^{\infty} \left(a_n^2(g) + b_n^2(g) \right).$$

Using the above fact, we see that our error can be quantified as

$$|f - \tilde{f}_N|_2^2 = \left(\int_a^b (f(x) - \tilde{f}_N(x))^2 dx \right)^{1/2} = \sum_{j=N+1}^{\infty} \left(a_j^2(f) + b_j^2(f) \right).$$

It is a well known fact that the Fourier coefficients of a function g will die off to zero as the index goes to infinity (the series would not converge otherwise). Hence, the squares of the coefficients must also go to zero. Therefore, for a large enough value for N, we expect to have quite minimal error, assuming we can compute the Fourier coefficients accurately.

5.2 An Outline of The Program

As stated before, our program will implement our previous calculations in the case where Ω is the unit circle (this makes the computation of the reciprocity gap integrals easier). For any given angle, the program will return the value of the function k at that angle. Our objective then is to first compute $\frac{\partial u^+}{\partial \mathbf{n}}$ and $[u]$, then divide these two quantities to generate the function k. To do so, we must compute their respective Fourier coefficients via. (11), (12), (24), and (25). Since $f(\pi) = f(-\pi)$, where f represents either the flux or the jump, we are able to use the following version of the trapezoid rule when numerically computing the reciprocity gap integrals in the (r, θ) coordinate system (see [3]):

$$\int_{-\pi}^{\pi} f(x)dx \approx \sum_{i=1}^{m} \left(\frac{f(-\pi + \frac{2(i-1)\pi}{m}) + f(-\pi + \frac{2i\pi}{m})}{2} \right) \frac{2\pi}{m}$$

$$
\begin{aligned}
&= \frac{2\pi}{m}\sum_{i=1}^{m-1}\frac{f(-\pi)+2f(-\pi+\frac{2i\pi}{m})+f(\pi)}{2} \\
&= \frac{2\pi}{m}\sum_{i=1}^{m-1}\frac{2f(-\pi)+2f(-\pi+\frac{2i\pi}{m})}{2} \\
&= \frac{2\pi}{m}\sum_{i=1}^{m} f(-\pi+\frac{2(i-1)\pi}{m}) \qquad (28)
\end{aligned}
$$

As input for the values of u and g in (8), we use a program which solves the forward problem, given the function k, for the temperature $u(r,\theta)$ at some pre-specified number of points on $\partial\Omega$. This gives us our values for u. What ever function g we use in the forward solver must also be used in the inverse solver – this specifies our choice of g. Since we only know the temperature u at a certain number of points on the $\partial\Omega$, this gives us the maximum value of m which can be used in (28). Since our test functions are defined in the (ρ,β) coordinate system, we had to use a change of coordinates to put them in the (r,θ) system. One can easily verify the following conversions between the two coordinate systems:

$$
\begin{aligned}
\rho(r,\theta) &= \sqrt{r^2-2r(x_0\cos(\theta)+y_0\sin(\theta))+x_0^2+y_0^2}, \qquad (29)\\
\beta(r,\theta) &= \arctan\left(r\sin(\theta)-y_0, r\sin(\theta)-x_0\right). \qquad (30)
\end{aligned}
$$

As stated in the last section, we cannot reconstruct our desired quantities as a full Fourier series; we must truncate our expansion at some value $n=N$ as in (27). The number of test functions N used for both the jump and the flux is specified by the user and will dramatically effect the quality of our reconstruction of k, as you will see in the next section. We now have all the information needed to reconstruction $\frac{\partial u^+}{\partial \mathbf{n}}$.

To finish the reconstruction of $[u]$, we must determine the constant term of its Fourier expansion. To do so, we determine where the flux changes signs and then call a routine that will find the corresponding zero of $\frac{\partial u^+}{\partial \mathbf{n}}$. This routine uses the secant method, a numerical method for finding roots that is similar to Newton's method. To find the root, the secant algorithm requires two initial guesses: we use the closest positive and negative value of the flux near the zero (see[3]). We can then determine the constant term by evaluating $[\widetilde{u}] = [u] - \frac{A_0}{2}$ at the zero, as was described earlier. However, due to computer rounding error, if we apply this procedure to each zero of the flux, we do not have a unique determination of the constant term as the theory suggests. To approximate this value, we use the negative of the average of

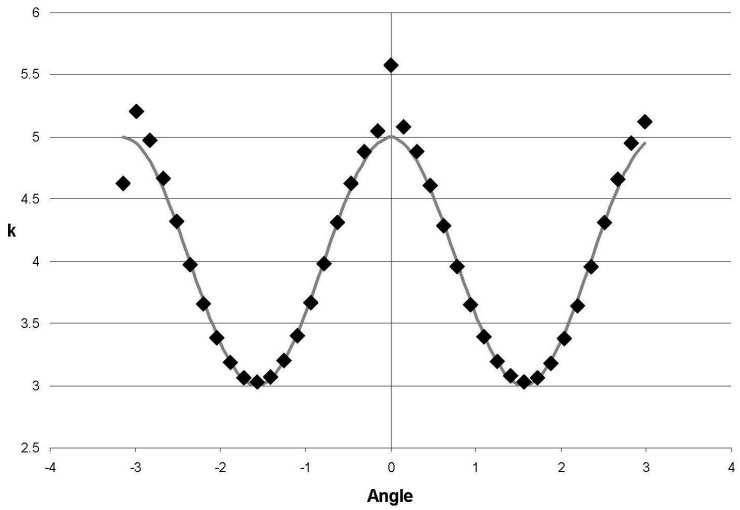

Figure 2: Reconstruction of $k = 4 + \cos(2\beta)$ on $[-\pi, \pi]$ using only the first four test-functions.

the determined values of $\frac{A_0}{2}$. We can now reconstruct $[u]$ as a truncated Fourier series and finally our function k.

5.3 Numerical Example

We now present an example where we take Ω to be the unit circle and D to be a circle of radius $R_D = 0.5$ centered at $(-0.25, 0.3)$. In our example, we take $g(r, \theta) = \sin(\theta)$ on $\partial\Omega$, $\alpha = 5$, and the true function k as being $4 + \cos(2\beta)$. Using a forward solver, we solve the forward problem for the temperature $u(r, \theta)$ at forty equally spaced nodes on $\partial\Omega$. We then use this information to compute the reciprocity gap integral of the needed test functions. Reconstructing the flux and the jump as in (13) and (23), respectively, we are able to recover our estimate of the function k on the interval $[-\pi, \pi)$ at forty nodes along ∂D, each spaced in angle measure (with respect to the (ρ, β) system) by $\frac{2\pi}{40}$.

Figure 2 shows our reconstruction of the given k. The solid line is the true k and the discrete points are our reconstructed values of k at the specified angle. Notice that our reconstruction involves only the first four terms of the Fourier series for both the jump and the flux. We have a very good estimate of the function k

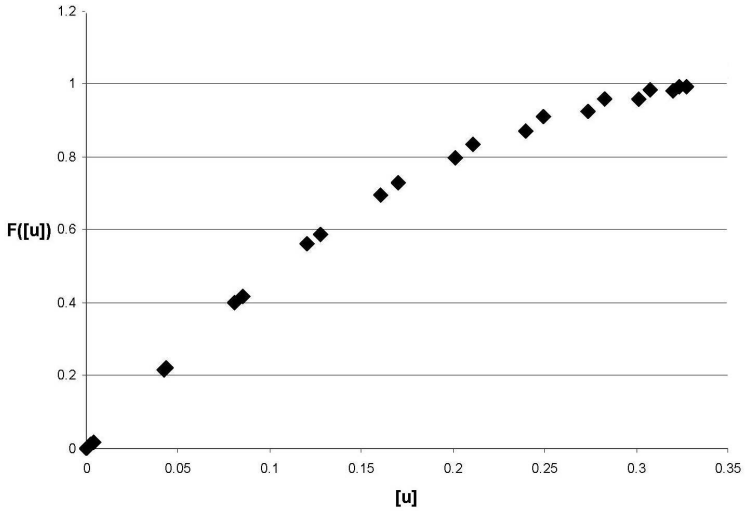

Figure 3: Reconstruction of $F([u])$ on the set of temperature jumps.

away from $\beta_0 = -\pi$ and $\beta_1 = 0$. This is because the jump is very near zero at β_0 and β_1, and thus we would expect to have problems there since we divided the flux by the jump to reconstruct k. Away from these points though, we have a very good approximation of k with an average relative error of only 1.51% (average relative error is defined as $\frac{1}{M}\sum_{i=1}^{M}\frac{\tilde{x}_i - x_i}{x_i}$, where $\tilde{x}_i$ is the approximate value, x_i is the true value, and M is the number of test points.) We can also reconstruct the function $F([u])$ on the set of temperature jumps by plotting the flux versus the jump (see Figure 3). Note that since F is odd, we show only the first quadrant in Figure 3.

Since we have such a good approximation of k taking only the first four terms of the Fourier series for the jump and the flux, from the above analysis on truncating the series at $n = N$, we expect to have even better results if we took the first eight terms of the series. This turns out not to be the case, however, as you can see in Figure 4 (the outliers at β_0 and β_1 were deleted for scaling purposes). Our average relative error went from 1.51% to about 49.2%. The reason for this is that this inverse problem is ill-posed, as will be quantified in the following section.

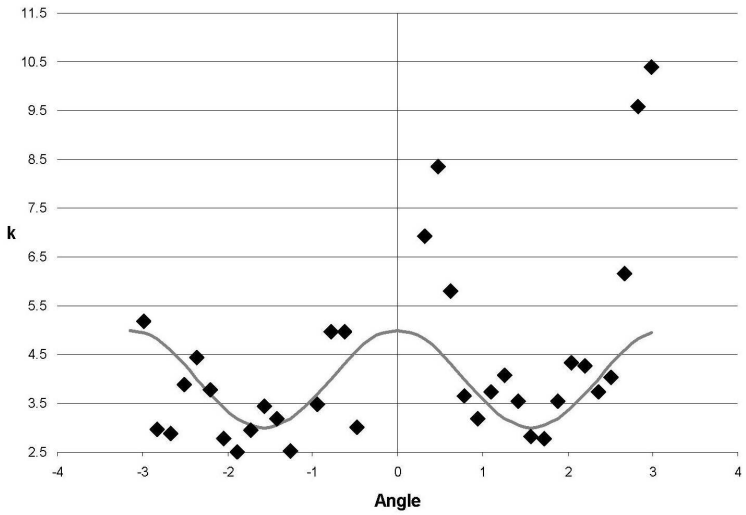

Figure 4: Reconstruction of $k = 4 + \cos(2\beta)$ on $[-\pi, \pi]$ using the first eight test functions.

6 Ill-Posedness

6.1 The Effects of Noise

In every practical application of mathematics, there is some level of error involved. In our case, since we are free to choose the flux on $\partial\Omega$, we will assume we know g exactly and that there is some error of magnitude ϵ in measuring u on the boundary of Ω. Thus, instead of measuring the actual value u, we are in fact measuring $\tilde{u} = u + \epsilon$ (if there is no noise from u, then there will always be some noise from computer roundoff error, which is what happened in our previous examples). As a result, or computed Fourier coefficients will also have some error: instead of computing the true coefficient a_j, we compute $\tilde{a}_j = a_j + e_j$, where e_j is some error. In virtually all inverse problems, the computation of $\tilde{a}_j$ becomes more and more unstable as j increases. In many cases, we find that

$$e_j \approx \frac{E}{R^j} \tag{31}$$

for some $R < 1$ and some constant E (as is true in the present case, which we show shortly).

From (31), it is clear that $|e_j|$ increases rapidly at high frequencies (large j). This means that for sufficiently large j, our estimate $\tilde{a}_j$ is comprised almost entirely of magnified noise and contains little information about the true value a_j. Using $\tilde{a}_j$ beyond this point is pointless, and in fact it completely destroys our estimate of the function we are trying to recreate. This is the *ill-posedness* of the inverse problem – certain information about the function we are trying to reconstruct using the $\tilde{a}_j$, especially high frequency "detail" information, is irretrievably corrupted by noise. This explains why when we chose large values for N in our example, our reconstructed k gave us no useful information about the true function.

We have seen that if we choose N to large in (27) we will have a lousy reconstruction. However, if we take N to be to small, then we won't have enough information about f to have a viable reconstruction. How do we handle this?

6.2 Regularization

There are various techniques one can use to attack this problem. Probably the most natural question to ask is "how do I choose N in order to get the best reconstruction of my unknown function?" Although this approach can easily be implemented, we decided to attack it from a different angle. Lets assume we have a function f (could be the flux or the jump) defined on the interval $[-\pi, \pi]$ with a Fourier series expansion as in (7). Instead of truncating our estimate of f, we expand f as an infinite series in the following manner:

$$\tilde{f}(x) = \frac{\tilde{a}_0(f)}{2} + \sum_{n=1}^{\infty}(\lambda(n)\tilde{a}_n(f)\cos(nx) + \psi(n)\tilde{b}_n(f)\sin(nx)), \tag{32}$$

where $\lambda(n)$ and $\psi(n)$ are weighting functions which decrease to zero at such a rate as to give us the most "useful" information about f. Note that we put no weighting factor on the first coefficient, $\tilde{a}_0$ (although we certainly could) since this coefficient is typically recovered quite stably. The use of an infinite series is valid here since, for large enough n, the weighting functions will be nearly zero so we can ignore the higher terms. The question now becomes how to choose the weighting functions λ and ψ?

Naturally, we wish to choose λ and ψ such that $|f - \tilde{f}_N|_2^2$ is a minimum (this will ensure that we have the best estimate of the true function f). Letting f have a Fourier expansion as in (7) and using (32), we see that $|f - \tilde{f}|_2^2$ is given by

$$\frac{a_0(f) - \tilde{a}_0(f)}{2} + \sum_{n=1}^{\infty}((a_n(f) - \lambda(n)\tilde{a}_n(f))\cos(nx) - (b_n(f) - \psi(n)\tilde{b}_n(f))\sin(nx))$$

$$= \frac{e_0}{2} + \sum_{n=1}^{\infty}(((\lambda(n)-1)a_n + \lambda(n)e_n)\cos(nx) + ((\psi(n)-1)b_n + \psi(n)d_n)\sin(nx))$$

$$= \frac{e_0^2}{2} + \sum_{n=1}^{\infty}((\lambda(n)-1)a_n + \lambda(n)e_n)^2 + ((\psi(n)-1)b_n + \psi(n)d_n)^2$$

where we have used the fact that $\tilde{a}_n = a_n + e_n$ and $\tilde{b}_n = b_n + d_n$, for small errors e_n and d_n, as well as Parseval's identity. It's simple to see that the choice of λ and ψ which minimizes this quantity (indeed, makes it zero except for the $e_0^2/2$ term) is given by

$$\lambda(n) = \frac{a_n}{a_n + e_n} \text{ and } \psi(n) = \frac{b_n}{b_n + d_n}.$$

These choices will leave $|f - \tilde{f}_N|_2^2 = \frac{e_0^2}{2}$. In the case where f is the flux, (26) implies that $a_0\left(\frac{\partial u^+}{\partial \mathbf{n}}\right) = 0$ and thus $e_0 = 0$. In the case where f is the jump, since we have computed the flux exactly, there will be no error in determining $A_0([u])$ using the procedure described earlier. Therefore, our choices for λ and ψ will then minimize the total error to zero in both cases.

The above choices for λ and ψ cannot be implemented as stated since a_n and b_n are unknown quantities (remember, we can only measure $\tilde{a}_n$ and $\tilde{b}_n$). Let's handle the a_n problem first. What we do know is that $\sum_j a_j^2 < \infty$ (this is a consequence of Parseval's identity). This implies that we can make a-priori estimates of a_j by using some sequence $\hat{a}_j$ with $\sum_j \hat{a}_j^2 < \infty$. A reasonable choice would be to use $\hat{a}_j = \frac{\tilde{a}_0}{j}$, which is a square integrable sequence with a modest rate of decay . We also have the problem that we have no information about e_n. In the next section, however, we will show that we can bound its magnitude as $|e_n| \leq E_n\bar{\epsilon}$, where $\bar{\epsilon}$ is the maximum error in measuring u on $\partial\Omega$ and E_n is some constant that will grow with n. We can use similar a-priori estimates for b_n and bound the magnitude of the corresponding error as $|d_n| \leq E_n\bar{\epsilon}$. Therefore, we can use these estimates and bounds to compute our weighting coefficients as

$$\lambda(j) = \frac{\hat{a_j}}{\hat{a_j} + E_j\bar{\epsilon}} \text{ and } \psi(j) = \frac{\hat{b_j}}{\hat{b_j} + E_j\bar{\epsilon}}.$$

Since E_j will grow as j gets larger, this implies that $\lambda(j)$ and $\psi(j)$ will decrease to zero as desired and, from construction,this should happen at such a rate as to give us the most useful information, filtering our most of the garbage due to the error in our measurements. This simple form of regularization (which is a type of Wiener

filtering (see [5])) will allow us to use arbitrarily large values of N in (27) and still have a reasonable reconstruction of the unknown function f. We will implement this scheme to reconstructing the flux and the jump on ∂D. Note, however, that if our error is noise free (*i.e.*, $\epsilon = 0$), then we are back with our original formulas with absolutely no regularization. However, computers always have some level of roundoff error and so for noiseless data, we can use a very small amount of error (say $\epsilon = 0.0001$) as a default for all of our computations.

6.3 Error Bounds

We now wish to verify our claims on the error bounds made in the last section in the cases where we are reconstructing the jump and the flux across ∂D. We again assume that u has some error ϵ when measured on $\partial\Omega$. Let's first consider the flux. From (11), we recall that the Fourier cosine coefficient of the flux is given by

$$a_n\left(\frac{\partial u^+}{\partial \mathbf{n}}\right) = \frac{-RG(v_n^c)}{2\,\pi\,R_d^{n+1}},\ \mathrm{n} \geq 0.$$

Therefore, we see that if u is measured with error ϵ on $\partial\Omega$, then the corresponding error in its Fourier cosine coefficient is quantified as

$$\begin{aligned}
|e_n| &= \frac{1}{2\pi R_D^{n+1}}\left|\int_{\partial\Omega}(u-\tilde{u})\frac{\partial v_n^c}{\partial \mathbf{n}}ds\right| \\
&= \frac{1}{2\pi R_D^{n+1}}\left|\int_{\partial\Omega}\epsilon\,\frac{\partial v_n^c}{\partial \mathbf{n}}ds\right| \\
&\leq \frac{1}{2\pi R_D^{n+1}}\int_{\partial\Omega}\left|\epsilon\,\frac{\partial v_n^c}{\partial \mathbf{n}}\right|ds \\
&\leq \frac{\bar{\epsilon}\,|\partial\Omega|}{2\pi R_D^{n+1}}\,\max_{\partial\Omega}\left(\frac{\partial v_n^c}{\partial \mathbf{n}}\right) \\
&= E_n\bar{\epsilon}
\end{aligned}$$

where $E_n = \frac{|\partial\Omega|}{2\pi R_D^{n+1}}\,\max_{\partial\Omega}\left(\frac{\partial v_n^c}{\partial \mathbf{n}}\right)$ is a constant and $\bar{\epsilon}$ is the maximum error incurred in measuring u on $\partial\Omega$.

Recall that (x_0, y_0) is the center of D, (r, θ) represents the standard polar coordinates as read from the origin, and (ρ, β) represents polar coordinates as read from (x_0, y_0). We wish to compute the maximum of the normal derivative (radial in the (ρ, β) system) of the function $v_n^c(\rho, \beta)$. By the chain rule and the triangle inequality,

we see that the normal derivative can be bounded by

$$\begin{aligned}\left|\frac{\partial v_n^c}{\partial \mathbf{n}}\right| &= \left|\frac{\partial v_n^c}{\partial \rho}\,\frac{\partial \rho}{\partial r} + \frac{\partial v_n^c}{\partial \beta}\,\frac{\partial \beta}{\partial r}\right| \\ &\leq \left|\frac{\partial v_n^c}{\partial \rho}\right|\,\left|\frac{\partial \rho}{\partial r}\right| + \left|\frac{\partial v_n^c}{\partial \beta}\right|\,\left|\frac{\partial \beta}{\partial r}\right|. \end{aligned} \tag{33}$$

By comparing (9) and (10), it is clear that the normal derivative of $v_n^s(\rho,\beta)$ also satisfies the above inequality.

Let $d = \sqrt{x_0^2 + y_0^2}$ be the distance from the origin (the center of Ω), to the center of D (the point (x_0, y_0)). From basic geometry, one can derive the following inequalities: $1 - d < \rho < 1 + d$ and $0 < R_D < 1 - d < 1$. Then from (9) we see that

$$\begin{aligned}\left|\frac{\partial v_n^c}{\partial \rho}\right|_{\partial\Omega} &= n\left|\rho^{n-1} - R_D^{2n}\rho^{-n-1}\right|\,|\cos(n\beta)| \\ &\leq n\left(\left|\rho^{n-1}\right| + R_D^{2n}\left|\rho^{-n-1}\right|\right) \\ &< n\left[(1+d)^{n-1} + (1-d)^{2n}(1+d)^{-n-1}\right] \\ &< n\left[(1+d)^{n-1} + (1+d)^{2n}(1+d)^{-n-1}\right] \\ &= 2n(1+d)^{n-1} \text{ and} \end{aligned} \tag{34}$$

$$\begin{aligned}\left|\frac{\partial v_n^c}{\partial \beta}\right|_{\partial\Omega} &= n\left|\rho^{n} - R_D^{2n}\rho^{-n}\right|\,|\sin(n\beta)| \\ &< 2n(1+d)^n. \end{aligned} \tag{35}$$

Notice that since $\rho(r,\theta)$ and $\beta(r,\theta)$ are independent of n (see (29) and (30)), we can simply bound their radial derivatives as positive constants. Therefore, using (33), (34) and (35), we can liberally set

$$\max_{\partial\Omega}\left(\frac{\partial v_n^c}{\partial \mathbf{n}}\right) = 2n(1+d)^n\left(\gamma + \frac{\sigma}{1+d}\right) \tag{36}$$

for some positive constants γ and σ. The same analysis can be done for the sine coefficient to show that $\max_{\partial\Omega} v_n^s$ can also be bounded by (36). Since $R_D < 1$, it follows that in this case E_n does grow with n and thus it's corresponding weighting functions will to decrease to zero, as desired. We can now choose arbitrarily large values for N when reconstructing the flux using the regularization procedure described in the previous section along with determination of E_n from this section.

All that is left now is to verify the claim in the case where we wish to reconstruct

$[u]$. Recall that the Fourier cosine coefficient for the jump is expressed as

$$A_n = \frac{RG(w_n^c)}{2n\pi R_D^n},\ \text{n} \geq 1.$$

As before, the error in calculating the Fourier cosine coefficient of $[u]$ can be expressed as

$$\begin{aligned} |e_n| &= \frac{1}{2n\pi R_D^n} \left| \int_{\partial\Omega} (u - \tilde{u}) \frac{\partial w_n^c}{\partial \mathbf{n}} ds \right| \\ &\leq \frac{\bar{\epsilon}\, |\partial\Omega|}{2n\pi R_D^n} \max_{\partial\Omega} \left(\frac{\partial w_n^c}{\partial \mathbf{n}} \right) \\ &= E_n' \bar{\epsilon} \end{aligned}$$

where $E_n' = \frac{|\partial\Omega|}{2n\pi R_D^n} \max_{\partial\Omega} \left(\frac{\partial w_n^c}{\partial \mathbf{n}} \right)$. We apply the same procedure as before and bound the normal derivative of w_n^c using the chain rule. This time we have

$$\begin{aligned} \left| \frac{\partial w_n^c}{\partial \rho} \right| &= n \left| \left(1 + \frac{1}{\alpha} \right) \rho^{n-1} - \left(\frac{1}{\alpha} - 1 \right) R_D^{2n} \rho^{-n-1} \right| |\cos(n\beta)| \\ &< n \left(1 + \frac{1}{\alpha} \right) \left| \rho^{n-1} - R_D^{2n} \rho^{-n-1} \right| \\ &< 2n \left(1 + \frac{1}{\alpha} \right) (1 + d)^{n-1} \text{ and} \\ \left| \frac{\partial w_n^c}{\partial \beta} \right| &= n \left| \left(1 + \frac{1}{\alpha} \right) \rho^{n} + \left(\frac{1}{\alpha} - 1 \right) R_D^{2n} \rho^{-n} \right| |\sin(n\beta)| \\ &< n \left(1 + \frac{1}{\alpha} \right) \left| \rho^{n} + R_D^{2n} \rho^{-n} \right| \\ &< 2n \left(1 + \frac{1}{\alpha} \right) (1 + d)^{n}. \end{aligned}$$

Since the choice of test functions will not have any change on the bounds for the radial derivatives of $\rho(r, \theta)$ and $\beta(r, \theta)$, we see that we can liberally set

$$\max_{\partial\Omega} \left(\frac{\partial w_n^c}{\partial \mathbf{n}} \right) = \left(1 + \frac{1}{\alpha} \right) \max_{\partial\Omega} \left(\frac{\partial v_n^c}{\partial \mathbf{n}} \right). \tag{37}$$

The same analysis can be done for the sine coefficient to show that $\max_{\partial\Omega} w_n^s$ can also be bounded by (37). This verifies that E_n' is a constant that grows with n and

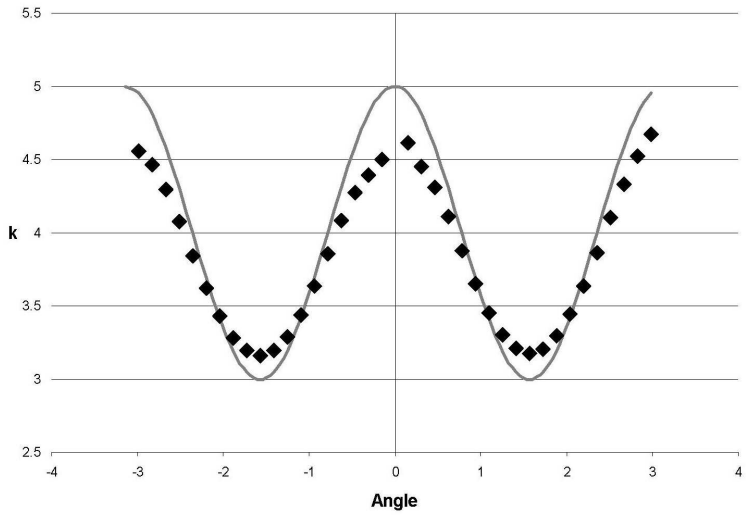

Figure 5: Reconstruction of $k = 4 + \cos(2\beta)$ with our regularization scheme implemented using 18 test-functions.

will therefore cause its corresponding weighting functions to decrease to zero. So we can choose arbitrarily large values for N when reconstructing the jump using the regularization procedure described in the previous section and with the above determination E'_n.

6.4 Numerical Example with Noise

We now turn back to the example in section 5.3. This time, we will implement the above regularization procedure into our computation of the series in our program. We can not *really* take as large of N as we like, however. If you take N to large, then the numbers get so small (or so large) that the computer can't handle them and returns horrible results, a simple consequence of floating point arithmetic. First, we will consider the case where there is no noise in our data, but we tell the program there is error of magnitude $\epsilon = 0.0001$ to account for any round off error. Figure 5 shows our reconstruction where we again take the first 18 terms of the series for the flux and the jump where we implement the above regularization procedure (compare with Figure 4).

Another case to consider is when there is noise in our measurements of u on

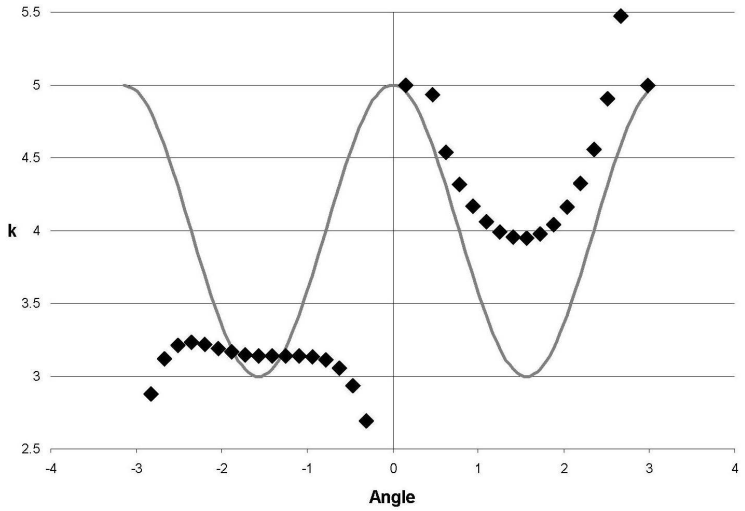

Figure 6: Reconstruction of k using 4 test-functions where there is noise in the data, but our regularization scheme is not implemented

$\partial\Omega$. This can be simulated in our forward solver by specifying the average level of noise you want added to your measurements. Figure 6 shows what happens when there is error in u of level $\epsilon = 0.005$ (to each of the 40 boundary measurements we add independent standard normal random errors with standard deviation 0.005) without the regularization procedure applied to our reconstruction (we have again deleted the major outliers for scaling purposes). Our reconstruction reveals little information about the actual k (the average relative error was 68.9%). By applying our regularization procedure to this example, our reconstruction improves dramatically if we tell the program that there is an error of magnitude $\frac{1}{10}\epsilon = 0.0005$ (the average relative error was reduced to only 15.7%). If we tell the program the error is of magnitude ϵ, then the weighting functions grow *too* fast and our estimate collapses to the average value of k. This implies that the estimates on E_n and E'_n made in the last section could probably be improved to give better results in general.

It seems that our regularization procedure could be improved upon when there is actual noise introduced into the data. But it works very well in letting us take a large number of test functions when there is no noise in our data (as long as we tell the inverse solver to account for any roundoff errors).

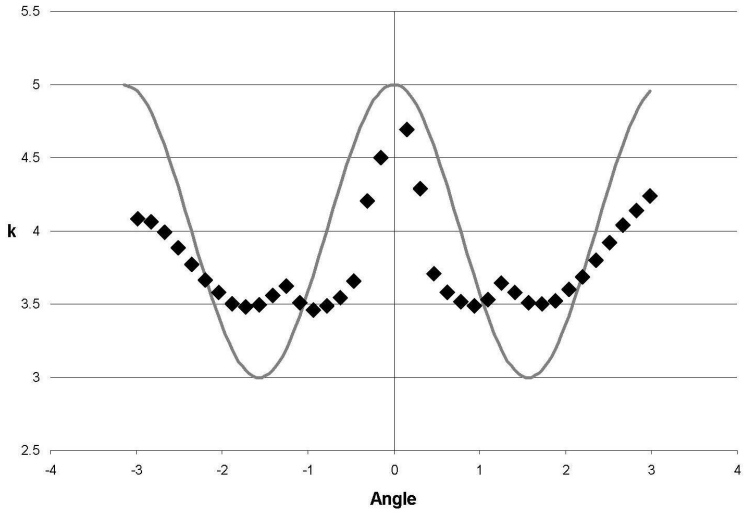

Figure 7: Reconstruction of k using 20 test-functions where there is noise in the data and our regularization scheme is applied to all reconstructions.

7 Nearly Circular Domains

We now wish to extend our results to the case where D is nearly circular. By nearly circular, we mean that D can be parameterized in the (r, θ) coordinate system as

$$D := \{(x(\theta), y(\theta) \in \Omega | x(\theta) = A + R_D(\theta)\cos(\theta),\ y(\theta) = B + R_D(\theta)\sin(\theta)\} \quad (38)$$

where $R_D(\theta) = R + \delta(\theta)$ for some function δ such that $0 \leq |\delta(\theta)| << 1$ and

$$R = \frac{1}{2\pi}\int_0^{2\pi} R_D(\theta)d\theta. \quad (39)$$

Our strategy will be to use our already existing theory by approximating D with a circular region $\bar{D}$ of radius R, as determined above, and whose center (x_0, y_0) is chosen to minimize the function

$$C(X, Y) = \int_0^{2\pi} \left((x(\theta) - (X + R\cos(\theta)))^2 + (y(\theta) - (Y + R\sin(\theta)))^2\right) dt. \quad (40)$$

In what follows, we will add the condition that $(\delta'(\theta))^2 \approx 0$ and let (ρ, β) represent polar coordinates as read from the center of $\bar{D}$.

7.1 Linearization

In order to extend our previous results, we will use a process called linearization. Since δ is small and $R < 1$, we will assume that $\delta^m \approx 0$ and $R^m\delta \approx 0$ for $m \geq 2$. As a result, when we compute ds on ∂D, we get

$$\begin{aligned} ds &= \sqrt{x'(\theta)^2 + y'(\theta)^2}\, d\theta \\ &= \sqrt{(R_D'(\theta)\cos(\theta) - R_D(\theta)\sin(\theta))^2 + (R_D'(\theta)\sin(\theta) + R_D(\theta)\cos(\theta))^2}\, d\theta \\ &= \sqrt{R_D'(\theta)^2 + R_D(\theta)^2}\, d\theta \\ &= \sqrt{\delta'(\theta)^2 + (R^2 + 2R\delta(\theta) + \delta(\theta)^2)}\, d\theta \\ &\approx \sqrt{R(R + 2\delta(\theta))}\, d\theta. \end{aligned} \tag{41}$$

We now wish to show how we can recover the flux in this nearly circular case. To do so, we will apply the above linearization process to determine the test functions and derivatives. The derivatives are easy. Since the radial derivatives of v_n^c and v_n^s were designed to be nearly zero near $\bar{D}$ in the (ρ, β) coordinate system (using R in place of R_D in our old test-functions), we will use the approximations

$$\frac{\partial v_n^c}{\partial \rho}(\mathbf{p}) \;\approx\; \frac{\partial v_n^s}{\partial \rho}(\mathbf{p}) \;\approx\; 0 \;\text{ for all }\; \mathbf{p} \in \partial D.$$

For the test functions, we have that on ∂D

$$\begin{aligned} v_n^c &= \left((R+\delta)^n + \frac{R^{2n}}{(R+\delta)^n}\right)\cos(n\beta) \\ &= \left(R^n + nR^{n-1}\delta + \frac{R^{2n}}{R^n + nR^{n-1}\delta}\right)\cos(n\beta) + O(\delta^2) \\ &= \left(R^n + nR^{n-1}\delta + \frac{R^n}{1 + \frac{n\delta}{R}}\right)\cos(n\beta) + O(\delta^2) \\ &= \left(R^n + nR^{n-1}\delta + R^n\left(1 - \frac{n\delta}{R}\right)\right)\cos(n\beta) + O(\delta^2) \\ &= 2R^n\cos(n\beta) + O(\delta^2) \end{aligned} \tag{42}$$

where we have used the approximation that if $|x|$ is small, then $\frac{1}{1+x} \approx 1 - x$. It follows that

$$RG(v_n^c) \approx -\int_{-\pi}^{\pi} 2R^n \frac{\partial u^+}{\partial \mathbf{n}} \sqrt{R(R+2\delta)}\cos(n\beta)d\theta$$

$$\approx -2\pi R^{n+1} a_n \left(\frac{\partial u^+}{\partial \mathbf{n}} \frac{\sqrt{R(R+2\delta)}}{R} \right), \text{ for } n \geq 0.$$

Similar computations can be done to recover estimates of the corresponding Fourier sine coefficient. We can therefore use (13) as our estimated reconstruction of the function $\frac{\partial u^+}{\partial \mathbf{n}} \frac{\sqrt{R(R+2\delta)}}{R}$, *i.e.*, we can reconstruct an estimate of $\frac{\partial u^+}{\partial \mathbf{n}} \frac{\sqrt{R(R+2\delta)}}{R}$ on D by reconstructing the flux on D'.

All that is left now is to reconstruct the jump. We start by reconstructing u^+. Using the same ideas from when we tried to reconstruct the flux, we will make the assumption that q_n^c and q_n^s are both zero on ∂D (since they were designed to be zero near $\partial \bar{D}$). The radial derivative of q_n^c can be computed in the exact same manor as when we computed (42), and we see that on ∂D

$$\begin{aligned}
\frac{\partial q_n^c}{\partial \rho} &= n \left((R+\delta)^{n-1} + \frac{R^{2n}}{(R+\delta)^{n+1}} \right) \cos(n\beta) \\
&= n \left(R^{n-1} + (n-1)R^{n-2}\delta + \frac{R^{n-1}}{1+\frac{(n+1)\delta}{R}} \right) \cos(n\beta) + O(\delta^2) \\
&= n \left(R^{n-1} + (n-1)R^{n-2}\delta + R^{n-1} - (n+1)R^{n-2}\delta \right) \cos(n\beta) + O(\delta^2) \\
&= 2nR^{n-1} \left(1 - \frac{\delta}{R} \right) \cos(n\beta) + O(\delta^2).
\end{aligned}$$

It follows that

$$\begin{aligned}
RG(q_n^c) &\approx \int_{-\pi}^{\pi} 2nR^{n-1} \left(1 - \frac{\delta}{R} \right) u^+ \sqrt{R(R+2\delta)} \cos(n\beta) d\beta \\
&\approx 2n\pi R^n \left(1 - \frac{\bar{\delta}}{R} \right) a_n \left(u^+ \frac{\sqrt{R(R+2\delta)}}{R} \right)
\end{aligned}$$

where $\bar{\delta}$ is the average value of $\delta(\beta)$. Since we chose R to be the average value of $R(\theta)$ on $[-\pi, \pi]$, see (39), it follows that

$$\bar{\delta} = \frac{1}{2\pi} \int_{-\pi}^{\pi} \delta(\beta) d\beta = \frac{1}{2\pi} \int_{-\pi}^{\pi} R(\beta) d\beta - \frac{1}{2\pi} \int_{-\pi}^{\pi} R d\beta = R - R = 0.$$

Therefore, we have that

$$a_n \left(u^+ \frac{\sqrt{R(R+2\delta)}}{R} \right) \approx \frac{RG(q_n^c)}{2n\pi R^n}, \text{ for } n \geq 1,$$

which is exactly (11). Similar computations can be carried out for the corresponding Fourier sine coefficient. We have now recovered everything needed to reconstruct $u^+\frac{\sqrt{R(R+2\delta)}}{R}$ except for the constant term a_0. We will take care of this as we did before after we reconstruct u^-. Note that we could have reconstructed the quantity $\left(1+\frac{\delta}{R}\right)u^+\frac{\sqrt{R(R+2\delta)}}{R}$ instead. However, this leads to major complications in computing the A_0 term for the jump. As long as δ is small, the approximation will be valid.

To reconstruct u^-, we turn back to (18) and use (19) and (20). Using our linearization process when substituting (19) into (18) yields

$$\int_{-\pi}^{\pi} n\alpha(R^{n-1}+(n-1)R^{n-2}\delta)u^-\sqrt{R(R+2\delta)}\cos(n\beta)$$

$$\begin{aligned}
&\approx n\alpha R^n\left(1+\frac{(n-1)\bar{\delta}}{R}\right)\int_{-\pi}^{\pi}u^-\frac{\sqrt{R(R+2\delta)}}{R}\cos(n\beta)d\beta\\
&\approx \int_{-\pi}^{\pi}(R^n+nR^{n-1}\delta)\left(\alpha\frac{\partial u^-}{\partial\mathbf{n}}\right)\sqrt{R(R+2\delta)}\cos(n\beta)d\beta\\
&= \int_{-\pi}^{\pi}R^n(1+\frac{n\delta}{R})\frac{\partial u^+}{\partial\mathbf{n}}\sqrt{R(R+2\delta)}\cos(n\beta)d\beta\\
&\approx \pi R^{n+1}\left(1+\frac{n\bar{\delta}}{R}\right)a_n\left(\frac{\partial u^+}{\partial\mathbf{n}}\frac{\sqrt{R(R+2\delta)}}{R}\right)\\
&\approx \frac{-RG(v_n^c)}{2}.
\end{aligned}$$

Notice that any terms involving δ and n must be pulled outside of the integrals in this case (so the reconstructed function has no dependence on n). Therefore, we have

$$a_n\left(u^-\frac{\sqrt{R(R+2\delta)}}{R}\right)\approx\frac{-RG(v_n^c)}{2n\pi\alpha R^n},\ \text{for } n\geq 1,$$

which is exactly (21). Similar computations show that the corresponding Fourier sine coefficients are given by (22). We are now in position to reconstruct the function $[u]\frac{\sqrt{R(R+2\delta)}}{R}$ as a Fourier series by determining the constant term $A_0\left([u]\frac{\sqrt{R(R+2\delta)}}{R}\right)$ as we did previously, *i.e.* by scaling A_0 so that the flux and the jump change signs

simultaneously. Hence, we can reconstruct the function $[u]\frac{\sqrt{R(R+2\delta)}}{R}$ using (23), and we are able to recover our desired quantity $k(\beta)$ using (3). Notice that the quantity $\frac{\sqrt{R(R+2\delta)}}{R}$ will cancel out when computing k. Therefore, by linearization, solving the posed inverse problem on D is approximated fairly well by solving it on the approximated circular region D'.

7.2 Numerical Example

As an example consider the inclusion $D \subset \Omega$ parameterized as in (38) with $A = B = 0$, and $R_D(\theta) = \frac{1}{5}\left(\frac{7}{2} + \frac{1}{2}\cos^2(\theta)\right)$, where Ω is again the unit disk. Using (39) and (40), we see that D is approximated by the circular inclusion D' of radius $R = 0.75$ and center at $(0, 0)$. Using a variation of our original forward solver, we are able to solve for the temperature $u(r, \theta)$ on $\partial\Omega$ given that $k = 4 + \cos(2\beta)$ and $g(r, \theta) = \sin(\theta)$. Even though there is no noise in our data, we tell the inverse solver there is an error of magnitude $\epsilon = 0.0005$ (to account for roundoff errors and the fact that D is *not* a circle). Figure 8 shows our reconstruction of the given k as described in the above section using twelve test-functions, as well as a graph of D and D' within Ω. The dotted line on the left represents the approximating circle D' and the solid line represents the true D. Our average relative error in this example was 10.4%.

As a second example, we take $A = B = 0$ and $R_D(\theta) = \frac{1}{4}\left(\frac{5}{2} + \frac{1}{20}\cos^3(\theta)\right)$ in (38) where Ω is still the unit circle. This time, (39) implies $R = 0.625$ and (40) implies we should take the center of D' to be $(0.048675, 0)$. Figure 9 shows our reconstruction of the same k, as well as a comparison of D and D'.

8 Inclusions of Unknown Location

We now address the following inverse problem: given the solution $u(r, \theta)$ on $\partial\Omega$ of (1)-(3) and that Ω and D have the same thermal conductivity $\alpha = 1$, determine the center of the inclusion D. We again assume that D is a circular inclusion centered at (a, b) in the (r, θ) system. Note that we are given no information about k. We start off by applying Green's second identity to both D and $\Omega \setminus D$ and adding them together to get

$$RG(v) = \int_{\partial\Omega} \left(u\frac{\partial v}{\partial \mathbf{n}} - vg \right) ds = \int_{\partial D} [u]\frac{\partial v}{\partial \mathbf{n}} ds$$

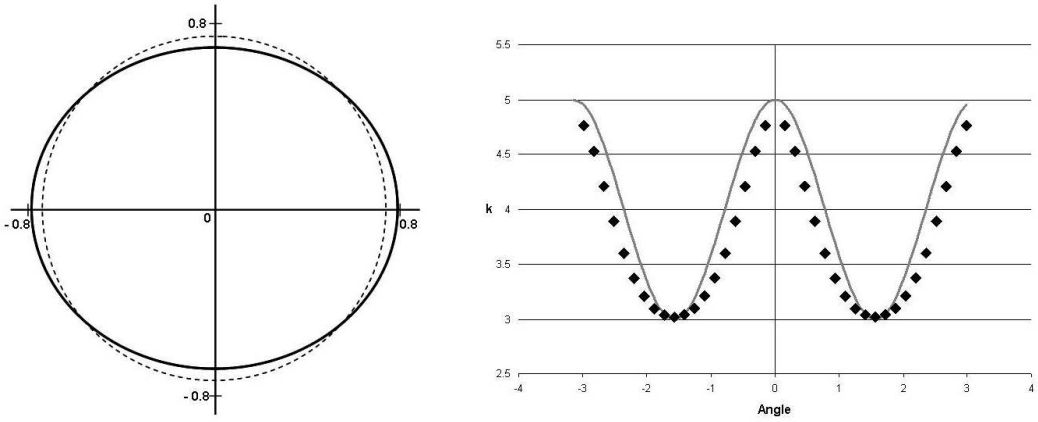

Figure 8: Left: Graph comparing D with D'. Right: Reconstruction of k.

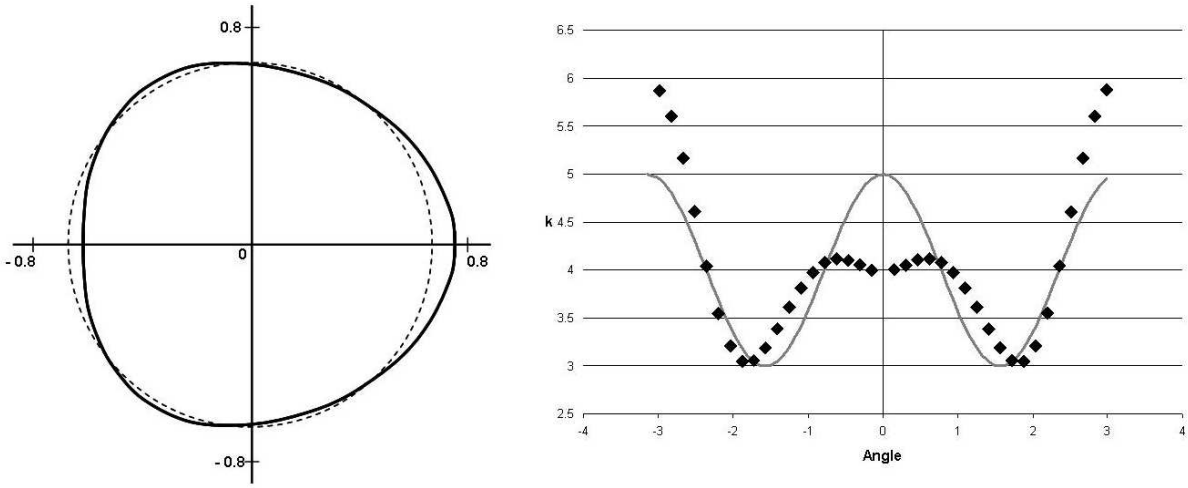

Figure 9: Left: Graph comparing D with D'. Right: Reconstruction of k.

where v is any function harmonic in all of Ω and u is a solution to (1)-(3). Again, we can compute $RG(v)$ for any given v.

Consider a (complex-valued) harmonic test function $v(x,y) = \frac{1}{\eta}e^{\eta(x+iy)}$, where η is any complex number. Note that $\nabla v = v\,\langle 1, i\rangle$. Using the parameterization of ∂D given by $x = a + R\cos(\theta)$, $y = b + R\sin(\theta)$, for $0 \le \theta \le 2\pi$, we find that

$$\begin{aligned} RG(\eta) &= Re^{\eta(a+bi)} \int_0^{2\pi} e^{R(\cos(\theta)+i\sin(\theta)} \langle 1, i\rangle \cdot \langle \cos(\theta), \sin(\theta)\rangle [u](\theta)d\theta \\ &= Re^{\eta(a+bi)} \int_0^{2\pi} e^{R(\cos(\theta)+i\sin(\theta)} e^{i\theta}[u](\theta)d\theta \end{aligned}$$

where we are thinking of RG as a function of η for the moment, and $[u]$ as a function of θ. If R is close to zero, then we can approximate (to first order)

$$RG(\eta) \approx Re^{\eta C^*} \int_0^{2\pi} e^{i\theta}[u](\theta)d\theta \tag{43}$$

since $e^{R(\cos(\theta)+i\sin(\theta))} = 1 + O(R)$. Here, we are using the notation $C^* = a + bi$ to denote the center of D.

For notational simplicity define $\phi(\eta) = RG(\eta)$, so that from (43) we have

$$\phi(\eta) = Je^{\eta C^*} \tag{44}$$

where $J = \int_0^{2\pi} e^{i\theta}[u](\theta)d\theta$ is the "jump integral." Recall also that we can compute $\phi(\eta)$ for any choice of $\eta \in \mathbb{C}$. We can also compute $\phi'(\eta)$, and indeed $\phi^{(j)}(\eta)$ for any $j \ge 1$, without differentiating the actual boundary data. We do this by defining

$$\phi^{(j)}(\eta) = RG\left(\frac{d^j}{d\eta^j}\left(\frac{1}{\eta}e^{\eta(x+iy)}\right)\right).$$

In particular, we point out that $\phi'(\eta) = C^* J e^{\eta C^*}$ so that

$$\frac{\phi'(\eta_0)}{\phi(\eta_0)} = C^*$$

for any $\eta_0 \in \mathbb{C}$. We have therefore recovered the center of D using only known boundary data.

From (44), this implies that we know the value of J as well. Future work needs to be done to determine the relationship between the integral J, the radius of D, and the value of k.

9 Conclusion and Future Extensions

In conclusion, we have shown how one can determine the levels of corrosion/disbonding which has incurred on the interface of two materials with presumably different thermal properties when one is completely contained within the other. We have shown how these ideas can be extended into an approximate solution to the inverse problem when D is nearly circular as well as addressed the issue of ill-posedness. However, through this work, we have found many new and exciting problems which need to be addressed in the future.

First, we would like to create a better method for solving the inverse problem in the nearly circular case, one that can be extended to general shapes for D. Our method relies heavily on the fact that D is a circular inclusion, so this might involve developing a completely new attack to the problem. One possible approach would be to use conformal mappings which map D into a circle (this is always possible by the Riemann Mapping Theorem as long as D is simply connected) and would extend to all of Ω, and then use our methods (see [1]).

Our method also relies on the fact that there is a *single* inclusion within Ω. We believe an important extension would be to solve the inverse problem when there are multiple inclusions within Ω. One possible method would include from complex analysis for designing families of test functions v_{ni}, each of which has a singularity at the center of the i^{th} inclusion. Then, maybe using the calculus of residues, one may be able to isolate one inclusion at a time in terms of boundary integrals on $\partial\Omega$.

Another interesting problem would be to use the time independent form of the heat equation:

$$\frac{\partial u}{\partial t} - \Delta u = 0$$

where t represents time (compare with (1)). This would involve considering the cases where you have data known for all time (continuous) about the temperature on $\partial\Omega$ as well as when you only have discrete information. Eventually, we hope the ideas we have discussed will be extended to the three-dimensional case where D now becomes a cylinder or a sphere contained within Ω.

References

[1] Ahlfors, Lars V., An Introduction to the Theory of Analytic Functions of One Complex Variable, 3 Ed., McGraw-Hill, 1979, pp. 229-232.

[2] Bryan, K. and Vogelius, M., A review of selected works on crack identification, *Geometric Methods in Inverse Problems and PDE Control*, IMA Volume 137, Springer-Verlag, pp. 25-46.

[3] Cheng, W. and Kincard, D., Numerical Mathematics and Computing, 5 Ed., Thomson, 2004, pp. 126-127.

[4] Marsden, Jarrold E. and Tromba, Anthony J., Vector Calculus, 4 Ed. Freeman, 2000, pp. 525-258.

[5] Johnson, Don H. and Dudgeon, Dan E., Array Signal Processing Concepts and Techniques, Prentice Hall, 1993, pp. 297-300.